International Journal of Thermodynamics (IJoT)
ISSN 1301-9724 / e-ISSN 2146-1511
www.ijoticat.com

Vol. 15 (No. 2), pp. 119-126, 2012
doi: 10.5541/ijot.374
Published online: May 16, 2012

Exergoeconomic Optimization of an Organic Rankine Cycle for Low-Temperature Geothermal Heat Sources

F. Heberle*, P. Bassermann, M. Preißinger and D. Brüggemann

Lehrstuhl für Technische Thermodynamik und Transportprozesse (LTTT),
Zentrum für Energietechnik (ZET), Universität Bayreuth,
Universitätsstraße 30, 95447 Bayreuth, Germany
LTTT@uni-bayreuth.de

Abstract

An exergoeconomic analysis of a geothermal power generation for a low-temperature resource is performed. An Organic Rankine Cycle (ORC) with isobutane and isopentane as working fluids is considered as binary power plant. A systematic parameter variation is done for the minimum temperature difference in the evaporator and condenser. The most suitable design parameters are evaluated under exergetic, economic and exergoeconomic criteria. The specific costs of electricity generation are minimal for the use of isobutane as working fluid and minimal temperature difference of 3 K at evaporation and 7 K at condensation. The most suitable concept for isopentane leads to only 0.4 % higher specific costs although the second law efficiency is 4.75 % lower. The exergoeconomic analysis permits to consider important criteria, like design and operating parameters in the fluid selection for ORC applications.

Keywords: *Organic Rankine Cycle; ORC; geothermal heat source; exergoeconomic analysis.*

1. Introduction

Geothermal power generation is a promising technology among the renewable energies. Depending on geothermal water temperature, different power plant concepts are suitable. In case of temperatures below 150 °C the Organic Rankine Cycle (ORC) or the Kalina Cycle are state-of-the-art technologies (DiPippo 2005). Several groups investigated the influence of ORC fluid selection on efficiency in case of low-temperature heat sources (Heberle & Brüggemann 2010; Mago et al. 2008; Madhawa Hettiarachchi et al. 2007; Saleh et al. 2007; Tchanche et al. 2009). Alternative optimization strategies, like supercritical cycles, were analyzed by Gu and Sato (Gu & Sato 2002) and Schuster et al. (Schuster, Karellas & Aumann 2010), showing a higher power output compared to subcritical cycles. Second law analyses of geothermal power plants were performed by Yari (Yari 2010) and Kanoglu (Kanoglu 2002). In order to combine an exergy analysis with economic aspects, the exergoeconomic method can be used (Bejan, Tsatsaronis, & Moran 1996; Erlach, Serra, & Valero 1999; Frangopoulos 1987; Lozano & Valero 1993; Tsatsaronis & Moran 1997). Exergoeconomic analyses are widely used to evaluate energy conversion processes and identify irreversibilities as well as optimization potentials (Abusoglu & Kanoglu 2009; Kwak, Kim, & Jeon 2003; Meyer et al. 2010; Petrakopoulou, Tsatsaronis & Morosuk 2010; Valero, Lozano & Bartolomé 1996; Zaleta-Aguilar, Rangel-Hernandez, & Royo 2010). In case of a geothermal medium temperature resource, Arslan (Arslan 2010) investigated the performance of the Kalina Cycle depending on geothermal water temperature and ammonia mass fraction under exergoeconomic criteria. The results show that in case of a present worth factor equal to 12 an ammonia concentration of 80 % and a geothermal outlet temperature of 90 °C is the optimal plant design.

In the mentioned investigations the minimum temperature difference in the heat exchanger, the so-called pinch point, was kept constant. The present study focuses on the exergoeconomic optimization of the ORC as a function of the pinch point at evaporation and condensation. To figure out the most suitable process parameter two ORC working fluids are compared for typical geothermal boundary conditions of the Southern German Molasse Basin located near Munich. As working fluids isopentane and isobutane are investigated, because they lead to significant efficiency differences, if a constant pinch point is assumed. In addition the fluids are often used in geothermal applications and show a low global warming potential.

2. Methods

2.1 ORC Model

A scheme of the geothermal ORC power plant is shown in Figure 1.

The working fluid is forced to higher pressure by a pump. The power applied by the pump can be determined by

$$P_{Pump} = \frac{\dot{m}_{ORC}(h_{2i} - h_1)}{\eta_{i,Pump}} \qquad (1)$$

where $\eta_{i,Pump}$ is the isentropic efficiency of the pump, $\dot{m}_{ORC}$ describes the mass flow rate of the ORC and h_1 and h_2 correspond to the enthalpy of working fluid at the inlet and outlet of the pump. The working medium is coupled to the geothermal water in the preheater and heated to saturation temperature. The energy balance of the preheater is given by

$$\dot{m}_{GW}(h_{GW,in} - h_{GW,out})_{PH} = \dot{m}_{ORC}(h_3 - h_2). \qquad (2)$$

*Corresponding Author : Tel.: +49 921 557161; fax: +49 921 557165

In this context $\dot{m}_{GW}$ corresponds to the mass flow of geothermal water, $h_{GW,in}$ and $h_{GW,out}$ to the enthalpy of geothermal water at the inlet and outlet of the preheater. In the next step the working fluid is evaporated without superheating. The energy balance of the evaporator represents

$$\dot{m}_{GW}(h_{GW,in} - h_{GW,out})_{EVP} = \dot{m}_{ORC}(h_4 - h_3). \quad (3)$$

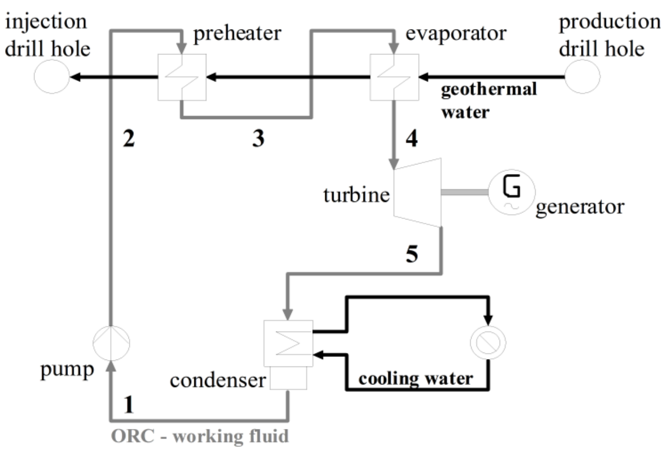

Figure 1.Scheme of a geothermal ORC power plant.

The vapour is expanded in a turbine. The power generated by the generator is given by

$$P_G = \eta_G \eta_{i,Turb} \dot{m}_{ORC}(h_5 - h_4) \quad (4)$$

where η_G is the efficiency of the generator. Finally the vapour is condensed by transferring the heat to the cooling water. The energy balance of the condenser is given by

$$\dot{m}_{CW}(h_{CW,out} - h_{CW,in}) = \dot{m}_{ORC}(h_5 - h_1) \quad (5)$$

where $\dot{m}_{CW}$ corresponds to the mass flow of the cooling medium and $h_{CW,in}$ and $h_{CW,out}$ to the enthalpy of the cooling medium at the inlet and the outlet of the condenser. All heat transfer processes are considered as isobaric changes of state and without heat losses to the environment. As an example the *T,s*-diagram for the ORC with isopentane as a working fluid is illustrated in Figure 2. The fluid properties are calculated using REFPROP (Lemmon, Huber, & McLinden 2002).
The outlet temperature of the geothermal water is chosen corresponding to maximum power output of the power plant.

2.2 Exergy analysis

To evaluate the cycle efficiency an exergetic analysis of the system is performed. The second law efficiency of the ORC is defined as

$$\eta_{II} = \frac{|P_G + P_{Pump}|}{\dot{E}_{GW}} \quad (6)$$

where P_G and P_{Pump} correspond to the power of the generator and the pump. The power for the pump of the cooling water cycle is not considered in the analysis. The absolute exergy flow $\dot{E}_{GW}$ is obtained by multiplying the specific exergy e_{GW} of the geothermal resource with the corresponding mass flow rate $\dot{m}_{GW}$:

$$e_{GW} = h - h_0 - T_0(s - s_0) \quad (7)$$

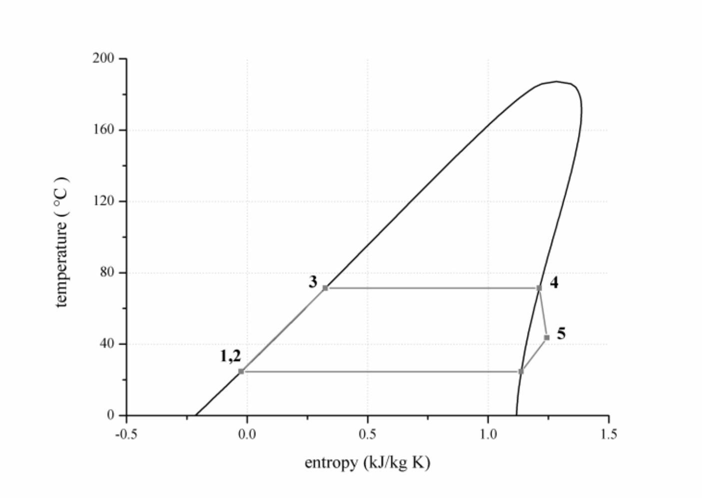

Figure 2. T,s-diagram of the working fluid isopentane.

In Equation 7 the subscript 0 corresponds to the reference state. In this case 15 °C and atmospheric pressure is chosen. Additionally an exergy balance is expressed for each considered component *k* of the system

$$\dot{E}_{F,k} = \dot{E}_{P,k} + \dot{E}_{L,k} + \dot{E}_{D,k} \quad (8)$$

where $\dot{E}_F$ and $\dot{E}_P$ describe the exergy flow rate of the fuel and the product. The exergy flow rate $\dot{E}_L$ includes heat losses to the surrounding or exergy that leaves the system in a physical way, like exhaust gases. The exergy flow rate $\dot{E}_D$ represents the exergy destruction rate associated with irreversibilities of heat transfer processes or friction. Exemplarily the exergy destruction rate of the preheater can be calculated as follows

$$\dot{E}_{D,PH} = \dot{m}_{ORC} T_0 \left[(s_3 - s_2) - \frac{h_3 - h_2}{T_{m,PH}} \right] \quad (9)$$

If a temperature difference of the heat source occurs, the thermodynamic mean temperature T_m for each component is calculated. To evaluate the inefficiencies of each component the exergy destruction ratio can be expressed as

$$y_{D,k} = \frac{\dot{E}_{D,k}}{\dot{E}_{GW}} \quad (10)$$

2.3 Economic analysis

The economic analysis is based on the purchased equipment costs (*PEC*) for each component of the system. Depending on heat exchanger surface area or turbine and pump power, the specific costs in US Dollar are calculated using an empiric correlation based on a large number of manufacturing data (Turton, Bailie, & Whiting 2003).

$$log_{10} PEC = K_1 + K_2 \, log_{10} X + K_3 (log_{10} X)^2 \quad (11)$$

The parameter K_1, K_2 and K_3 for the considered components are listed in Table 1.

The power of the pump and the turbine are determined by the process simulations. The heat exchanger surface for the preheater, evaporator and condenser is calculated assuming an ideal counter current flow (Baehr & Stephan 2004; Böckh 2006). Regarding the specific costs for plate heat exchanger, the required surfaces are multiplied with correction factors according to the NTU-Method determined by the VDI Wärmeatlas chapter Ca1-Ca6 (VDI-Gesellschaft Verfahrenstechnik und Chemieingenieurwesen 2006). Therefore a plate heat exchanger with two passes for the geothermal water flow and four passes for the ORC working fluid is considered.

Table 1. Constants K_1, K_2 and K_3 according to Equation 10 for different system components (Turton, Bailie, & Whiting 2003).

component	**Variable *X* (unit)**	K_1	K_2	K_3
pump	power (kW)	3.3892	0.0536	0.1538
preheater	area (m²)	4.6656	-0.1557	0.1547
evaporator	area (m²)	4.6656	-0.1557	0.1547
steam turbine	power (kW)	2.6259	1.4398	-0.1776
condenser	area (m²)	4.6656	-0.1557	0.1547

The annual capital investment cost rate $\dot{Z}_{CI}$ of the whole plant is calculated by

$$\dot{Z}_{CI} = \frac{6{,}32}{h_O} \cdot \sum_K PEC_K \cdot \frac{i \cdot (1+i)^n}{(1+i)^n - 1} \tag{12}$$

where the interest rate i is assumed to be moderate at 5 % and the economic life n of the plant is 20 years. The annual operating hours h_O of the geothermal power plant were supposed to be 7500 h. The annual cost expense concerning operation and maintenance Z_{OM} is estimated to be 20 % of PEC for the whole system.

$$Z_{OM} = 0.2 \cdot \sum_K PEC_K \tag{13}$$

2.4 Exergoeconomic analysis

The exergoeconomic analysis combines exergetic and economic aspects. The objectives of the method are the identification of the location and magnitude of exergy losses and exergy destruction. The associated costs for the streams in any plant component are calculated. In consequence each component can be evaluated according to the cost formation of the product separately. For the analysis in the present work the proposed method by Tsatsaronis and Winhold (Tsatsaronis &Winhold 1985) is used. The so-called exergy costing converts an exergy stream $\dot{E}_i$ to a cost stream $\dot{C}_i$, by multiplying the exergy with a corresponding factor c_i:

$$\dot{C}_i = c_i \cdot \dot{E}_i \tag{14}$$

A system of equations is set up consisting of the cost balance for each component of system:

$$\dot{C}_{P,k} = \dot{C}_{F,k} - \dot{C}_{L,k} + \dot{Z}_K \tag{15}$$

The factor $\dot{Z}_K$ describes the average cost of a component as a function of the operation and maintenance costs and the PEC:

$$\dot{Z}_K = \left(\dot{Z}_{OM} + \dot{Z}_{CI}\right) \cdot \frac{PEC_K}{\sum_K PEC_K} \tag{16}$$

The unknown variables c_i of each single flow can be determined by solving the system of equation by using auxiliary equations. Regarding the cost rate of the fuel in case of geothermal power generation, the electricity cost rate of the borehole pump $\dot{C}_{bh,pump}$ and the investment costs for drilling Z_{dr} as well as the borehole pump $Z_{bh,pump}$ have to be considered.

$$\dot{C}_{Fuel} = \dot{C}_{bh,pump} + \frac{Z_{dr} + Z_{bh,pump}}{h_O} \cdot \frac{i \cdot (1+i)^n}{(1+i)^n - 1} \tag{17}$$

Drilling and borehole pump costs are assumed to be 9.5 Mio$. For the evaluation of the system and its components important exergoeconomic coefficients should be introduced. The relative cost difference r_K of a component is defined as

$$r_K = \frac{c_{P,K} - c_{F,K}}{c_{F,K}} \tag{18}$$

The exergoeconomic factor f_K is expressed as

$$f_K = \frac{\dot{Z}_K}{\dot{Z}_K + c_{F,K}\left(\dot{E}_{F,K} - \dot{E}_{P,K}\right)} \tag{19}$$

The optimization criteria for the system is to minimize the total specific cost rate of the product $c_{P,total}$

$$c_{P,total} = \frac{\dot{C}_{P,total}}{\dot{E}_{P,total}} = \frac{(c_{Fuel,total} E_{Fuel,total} + \sum_K \dot{Z}_K)}{\dot{E}_{P,total}} \tag{20}$$

According to constant geothermal conditions and variable power output of the geothermal power plant $c_{p,total}$ should be preferred as a variable to optimize the system compared to the total cost rate of the product $\dot{C}_{P,total}$.

3. Results and Discussion

For the steady-state simulations the parameters of the geothermal resource and the cooling water, listed in Table 2, are set as constant.

By adapting the pressures p_1 and p_2 the pinch point of the condensation is varied between 1 K and 12 K and in case of evaporation in the range of 1 K to 15 K. Hence, for each working fluid 180 calculations are performed. In order to illustrate limitation of process in terms of the minimum temperature difference in the heat exchangers Figure 3a shows the $T, \mathrm{d}\dot{H}$ -diagram for isopentane and 5 K for the minimum temperature difference at evaporation $\Delta T_{PP,EVP}$ and condensation $\Delta T_{PP,C}$.

Table 2. Parameters for geothermal conditions and cooling water.

parameter	
inlet temperature of the geothermal water $T_{GW,in}$ (°C)	120
mass flow of the geothermal water $\dot{m}_{GW}$ (kg/s)	65.5
pressure of the geothermal water p_{GW} (bar)	15
inlet temperature of the cooling water $T_{CW,in}$ (°C)	15
outlet temperature of the cooling water $T_{CW,out}$ (°C)	20

3.1 Exergy analysis

The $T, \mathrm{d}\dot{H}$ -diagram in Figure 3b shows the ORC in case of isobutane as working fluid. The boundary conditions are equal to Figure 3a. The process pressures are chosen according to the maximum power output. In comparison to isopentane the use of isobutane leads to a 1.4 K lower outlet temperature of the geothermal water. In consequence 471 kW more exergy is transferred to the ORC process and the second law efficiency is 3.3 % in the case of isobutane.

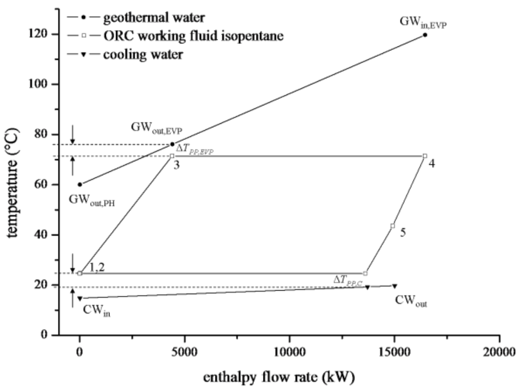

Figure 3a. $T, d\dot{H}$ -diagram of the geothermal ORC with isopentane as a working fluid.

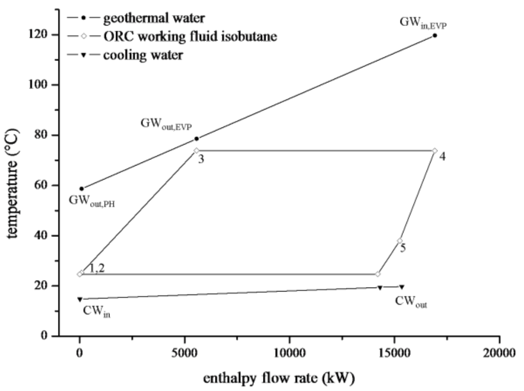

Figure 3b. $T, d\dot{H}$ -diagram of the geothermal ORC with isobutane as a working fluid.

In Figure 4 the second law efficiency of the ORC with isobutane and isopentane as a working fluid is shown as a function of the temperature difference at the pinch point at evaporation.

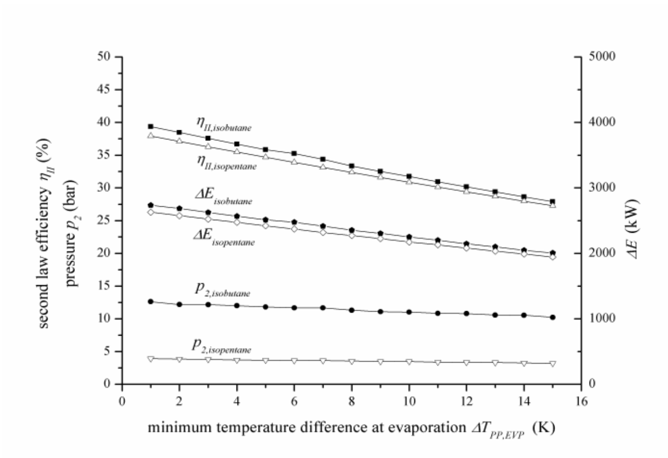

Figure 4. Second law efficiency, condensation pressure and transferred exergy of isobutane and isopentane as a function of the pinch point at evaporation ($\Delta T_{PP,C}$ = 5 K).

The pinch point at condensation $\Delta T_{PP,C}$ = 5 K is kept constant. Additionally the maximum cycle pressure p_2 and the transferred exergy $\Delta\dot{E} = \dot{E}_4 - \dot{E}_2$ are plotted. The process pressure p_2 is decreasing with rising temperature difference, because a lower pressure leads to a lower saturation temperature T_3. In consequence a higher temperature difference at the pinch point leads to a lower pressure ratio at the expansion and the second law efficiency decreases. In addition less exergy is transferred to the cycle with rising temperature difference. The use of isobutane as a working fluid is up to 3.76 % more efficient compared to isopentane. For a more detailed analysis the exergy values of four exemplary case studies are listed in Table 3.

Table 3. Results of the exergy analysis for isobutane and isopentane as ORC working fluids and different minimum temperature differences in the evaporator and condenser.

	isobutane (5 K / 5 K)	isobutane (3 K / 7 K)	isopentane (5 K / 5 K)	isopentane (3 K / 6 K)
P_T (kW)	1638.72	1638.81	1532.13	1564.52
P_{net} (kW)	1558.28	1554.34	1508.51	1539.42
$\dot{m}_{ORC}$ (kg/s)	43.13	43.62	39.36	39.69
$\dot{m}_{CW}$ (kg/s)	729.59	733.73	713.42	719.77
p_1 (bar)	11.82	12.35	3.69	3.88
p_2 (bar)	3.47	3.68	0.90	0.94
T_1 (°C)	24.66	26.65	24.57	25.55
T_3 (°C)	73.86	75.94	71.38	73.29
η_{II} (%)	35.83	35.74	34.69	35.40
$\dot{E}_{D,PH}$ (kW)	273.78	245.80	235.92	221.06
$\dot{E}_{D,EVP}$ (kW)	638.99	582.63	716.85	661.54
$\dot{E}_{D,Turb}$ (kW)	423.96	421.42	390.11	396.67
$\dot{E}_{D,C}$ (kW)	385.38	486.08	389.37	442.84
$\dot{E}_{D,Pump}$(kW)	14.83	15.06	5.70	6.00
$\dot{E}_{D,total}$(kW)	1736.94	1750.98	1737.94	1728.10
$y_{D,PH}$ (%)	7.99	7.15	6.99	6.51
$y_{D,EVP}$ (%)	18.65	16.95	21.24	19.48
$y_{D,Turb}$ (%)	12.38	12.26	11.56	11.68
$y_{D,C}$ (%)	11.25	14.14	11.54	13.04
$y_{D,Pump}$ (%)	0.43	0.44	0.17	0.18
$y_{D,total}$ (%)	50.70	50.95	51.50	50.88

In case of a higher pinch point at the condensation the differences in efficiency rise. The use of isobutane is 4.75 % more efficient for $\Delta T_{PP,C} = 7$ K compared to isopentane as working fluid and $\Delta T_{PP,C} = 6$ K. For all concepts the highest exergy destruction rate is observed in the evaporator. In case of the turbine, as well as in case of the pump, the higher mass flow rate of ORC with isobutane as a working fluid leads to higher irreversibilities in these components. Compared to the exergy destruction rate of the evaporator, the condenser shows lower values for both working fluids. The differences can be explained with the help of Figure 3. The mean temperature of the geothermal water and ORC working fluid in case of evaporation differs significantly compared to the mean temperature of cooling water and ORC working fluid in case of condensation. The exergy losses would be zero, when the curves of the heat source or sink and the ORC would match each other. The total exergy destruction rate is minimal for isopentane with $\Delta T_{PP,C} = 6$ K and $\Delta T_{PP,EVP} = 3$ K. Also the exergy destruction ratio y_D shows that a higher temperature difference at the pinch point is less efficient.

3.2 Economic analysis

In Figure 5 the surface area of the evaporator and the condenser is plotted as a function of temperature difference at the pinch point.

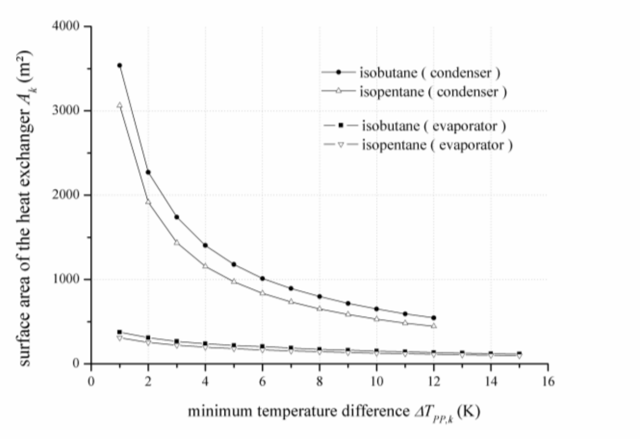

Figure 5. Surface area of the evaporator and condenser depending on temperature difference at the pinch point.

As expected, the surface area for both heat exchangers increases with decreasing temperature difference. The required surface of the evaporator is lower and the slope of the increase is less steep compared to the condenser. This is due to a lower amount of heat transferred to the ORC and a higher logarithmic mean temperature difference in the case of the evaporator. For isobutane as a working fluid, the injection temperature of the geothermal water is about 2 K lower compared to isopentane. For this reason a 4 % higher amount of heat is transferred to the ORC compared to isopentane. In consequence the surface area of the evaporator and the condenser is up to 23 % higher. Additionally the influence of heat transfer properties, like thermal conductivity, lead to a higher heat transfer coefficient in the case of isopentane compared to isobutane. In Table 4 the heat exchanger surface areas and the PECs of each component are listed for the chosen case studies. The use of isobutane leads to more than 7 % higher total PECs of the power plant components compared to isopentane. According to the calculated surface areas the condenser is the most expensive component of the system.

Table 4. Results of the economic analysis for isobutane and isopentane as ORC working fluids and different minimum temperature differences in the evaporator and condenser.

	isobutane (5 K / 5 K)	isobutane (3 K / 7 K)	isopentane (5 K / 5 K)	isopentane (3 K / 6 K)
A_{PH} (m²)	504.5	563.46	375.69	475.69
A_{EVP} (m²)	216.6	238.09	179.77	218.21
A_C(m²)	1177.0	912.48	972.55	855.02
PEC_{PH} ($)	237106.8	255825.82	195129.44	227845.31
PEC_{EVP} ($)	139912.7	147716.26	126180.48	140505.81
PEC_{Turb} ($)	262419.2	260513.62	257122.25	258777.85
PEC_C ($)	514892.5	363343.11	381490.68	345914.72
PEC_{Pump} ($)	12484.4	12600.10	6133.56	6323.98
PEC_{total} ($)	1166815.5	1039998.91	966056.40	979367.68

3.3 Exergoeconomic Analysis

Figure 6 shows the specific costs of the product as a function of minimal temperature difference of the evaporator using isobutane and isopentane as an ORC working fluid. According to the cost minima, the pinch point of the condenser is plotted for each operating point.

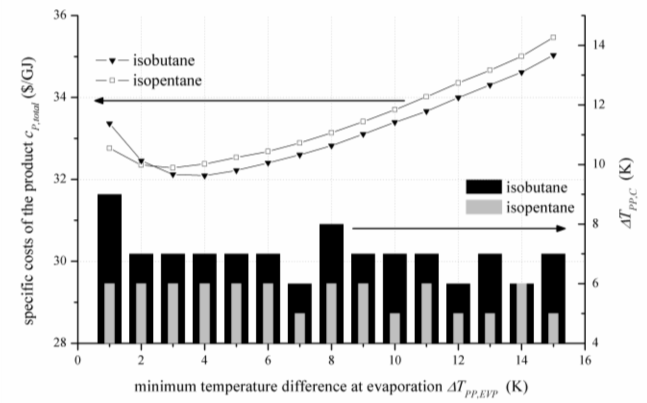

Figure 6. Specific costs of the product and corresponding pinch points at condensation as a function of temperature difference at evaporation.

In the case of isobutane, the design parameters $\Delta T_{PP,EVP} = 3$ K and $\Delta T_{PP,C} = 7$ K lead to minimal costs for electricity with $c_{p,total} = 32.14$ \$/GJ. Using isopentane as a working fluid, $\Delta T_{PP,EVP} = 3$ K and $\Delta T_{PP,C} = 6$ K are the most suitable operating parameters under exergoeconomic criteria. Compared to isobutane, the specific costs of electricity are only 0.4 % higher, although the second law efficiency is 4.75 % lower. The results of the detailed exergoeconomic analysis are listed in Table 5.

The results are based on a lifetime of 20 years for all ORC components. For the preheater the relative cost difference r_{PH} and the exergoeconomic factor f_{PH} show significantly high values. In this case it should be attempted to reduce the capital investment costs of the component at the expense of efficiency (Bejan, Tsatsaronis, & Moran 1996). Since the efficiency of the preheater in the considered cases is directly coupled to the minimum temperature difference at evaporation such a procedure leads to a significant decrease of the efficiency of the whole system. The other system components show typical values for the exergoeconomic factor depending on the different types like heat exchanger, turbine or pump.

Table 5. Results of the exergoeconomic analysis for isobutane and isopentane as ORC working fluids and different minimum temperature differences in the evaporator and condenser.

	isobutane (5 K /5 K)	isobutane (3 K / 7 K)	isopentane (5 K / 5 K)	isopentane (3 K / 6 K)
r_{PH} (%)	201.52	214.79	225.99	235.27
r_{EVP} (%)	61.04	60.59	62.22	60.56
r_{Turb} (%)	38.79	38.47	40.05	39.45
r_C (%)	-	-	-	-
r_{Pump} (%)	44.12	43.17	72.97	71.31
f_{PH} (%)	76.86	81.84	76.92	80.63
f_{EVP} (%)	45.64	51.38	41.49	46.17
f_{Turb} (%)	33.30	33.15	36.42	35.72
f_C (%)	-	-	-	-
f_{Pump} (%)	49.71	50.69	57.04	56.57
$c_{p,PH}$ ($/GJ)	20.70	21.61	22.38	23.02
$c_{p,EVP}$ ($/GJ)	11.06	11.03	11.14	11.02
$c_{p,Turb}$($/GJ)	45.30	46.78	44.58	45.38
$c_{p,C}$ ($/GJ)	-	-	-	-
$c_{p,Pump}$ ($/GJ)	32.32	32.10	38.79	38.41
$c_{p,total}$($/GJ)	33.10	32.14	32.56	32.26

Concerning the sensitivity of the results due to the economic boundary conditions a case study for the interest rate is performed. An increase to 8 % lead to a higher cost rate of the fuel c_{Fuel} and a higher specific cost rate of the product $c_{P,total}$. In the case of isobutane as working fluid and a pinch point of 5 K at evaporation and condensation the specific cost rate increases up to 20 % in comparison to an interest rate of 5 %. For the same process parameters the influence of the heat transfer areas on the specific cost rate of the product is calculated. A comparison of correlations and experimental data for the heat transfer coefficient shows typical uncertainties of 20 %. Assuming 20 % higher heat transfer areas for the preheater, evaporator and condenser the specific cost rate of the product increases up to 6.2 %.

4. Conclusions

In this paper an exergoeconomic analysis of a geothermal power generation for a low-temperature resource is performed. The results show that the method is useful to identify the most favourable design parameters of the evaporator and condenser. Compared to common investigations the minimum temperature difference in the heat exchanger is not kept constant. An exergetic, economic and exergoeconomic analysis is done for isobutane and isopentane as ORC working fluids. Finally the specific costs of electricity generation are calculated by a systematic variation of the minimum temperature difference in the heat exchangers. Using isobutane as a working fluid leads to higher second law efficiency compared to isopentane. For both fluids, the highest irreversibilities occur in the evaporator, due to a high mean temperature difference between geothermal water and ORC working fluid. The highest surface of the heat exchanger equipment is identified for the condenser. As a result the condenser is the most expensive component of the system. The choice of isobutane as a working fluid leads to lower heat transfer coefficients compared to isopentane, mainly caused by transport properties of the working fluid. Under exergoeconomic criteria isobutane with a minimum temperature difference of 3 K at evaporation and 7 K at condensation is to favour. The most suitable concept for isopentane leads to only 0.4 % higher specific costs although the second law efficiency is 4.75 % lower. The differences for the specific costs are relatively low because of the high investment costs concerning the exploration of the geothermal reservoir. The costs for drilling are 8 times higher than the PECs for the main components of the power plant. In addition the sensitivity of the results in dependence of heat transfer correlations and interest rate is quantified. An increase of 20 % for heat transfer areas lead to a 6.2 % higher specific cost rate of the product. To investigate this aspect in detail a comparison of different heat exchanger designs and heat transfer correlations will be performed in a the next step.

5. Further work

Different optimization concepts, like zeotropic fluid mixtures as ORC working fluids or supercritical cycles, will be investigated under exergoeconomic criteria in near future. Additionally the ORC in the case of waste heat recovery will be considered. For this application the costs for the exploitation of the heat source are significant lower compared to geothermal power plants. Therefore the difference in fluid selection due to different heat transfer areas and exergoeconomic aspects will be more crucial.

Nomenclature

A	surface area (m^2)
c	specific cost ($/GJ)
C	cost rate ($/h)
$\dot{E}$	exergy rate (kW)
f	exergoeconomic factor (%)
h	enthalpy (kJ/kg)
$\dot{H}$	enthalpy flow rate (kW)
$\dot{m}$	mass flow rate (kg/s)
p	pressure (bar)
P	mechanical power (kW)
$\dot{q}$	heat flux (kJ/s)
r	relative cost difference (%)
s	entropy (kJ/kgK)
T	temperature (K)
y	exergy destruction ratio
$\dot{Z}$	annual cost rate ($/%)

Greek letters

η	efficiency
ΔT	temperature difference (K)

Subscripts

0	ambient conditions
1-5	state points of the cycle
II	second law
C	condenser
CW	cooling water
D	destruction
EVP	evaporator
F	fuel
G	generator
GW	geothermal water
in	inlet
k	number of system component
L	losses
out	outlet

net	net
P	product
PP	pinch point
Pump	pump
PH	preheater
s	isentropic
Turb	turbine
total	total

Acronyms

ORC	Organic Rankine Cycle
PEC	purchased equipment cost

References

Abusoglu, A., & Kanoglu, M. (2009). Exergoeconomic Analysis and Optimization of Combined Heat and Power Production: A Review. *Renewable and Sustainable Energy Reviews*, 13(9), 2295-2308.

Arslan, O. (2010). Exergoeconomic Evaluation of Electricity Generation by the Medium Temperature Geothermal Resources, Using a Kalina Cycle: Simav Case Study. *International Journal of Thermal Sciences, 49*(9), 1866–1873.

Baehr, H. D., & Stephan K. (2004). *Wärme- und Stoffübertragung*, (4th ed.). Berlin, Spinger-Verlag.

Bejan, A., Tsatsaronis, G., & Moran M. (1996). *Thermal Design & Optimization*, New York, John Wiley & Sons.

Böckh, P. (2006). *Wärmeübertragung*, (2nd ed). Berlin, Springer-Verlag.

DiPippo, R. (2005). *Geothermal Power Plants*, (2nd ed). Oxford, Elsevier Science.

Erlach, B., Serra, L., & Valero, A. (1999). Structural Theory as Standard for Thermoeconomics. *Energy Conversion and Management*, *40*(15-16), 1627–1649.

Frangopoulos, C. A. (1987). Thermo-economic Functional Analysis and Optimization. *Energy, 12*(7), 563–571.

Gu, Z., & Sato, H. (2002). Performance of Supercritical Cycles for Geothermal Binary Design. *Energy Conversion and Management, 43*(7), 961–971.

Heberle, F., & Brüggemann, D. (2010) Exergy Based Fluid Selection for a Geothermal Organic Rankine Cycle for Combined Heat and Power Generation. *Applied Thermal Engineering*, *30*(11-12), 1326–1332.

Kanoglu, M. (2002). Exergy Analysis of a Dual-level Binary Geothermal Power Plant. *Geothermics*, *31*(6), 709–724.

Kwak, H.-Y., Kim, D.-J., & Jeon, J.-S. (2003). Exergetic and Thermoeconomic Analyses of Power Plants. *Energy, 28*(4), 343–360.

Lemmon, E.W., Huber, M. L., & McLinden, M.O. (2002). *NIST Standard Reference Database 23 – Version 8.0.* Physical and Chemical Properties Division. National Institute of Standards and Technology, Boulder, Colorado, US Department of Commerce, USA.

Lozano, M. A., & Valero, A. (1993). Theory of the Exergetic Cost. Energy *18*(9): 939–960.

Madhawa Hettiarachchi, H. D., Golubovic, M., Worek, W.M., & Ikegami, Y. (2007). Optimum Design Criteria for an Organic Rankine Cycle Using Low-temperature Geothermal Heat Sources. *Energy, 32*(9), 1698–1706.

Mago, P. J., Chamra, L. M., Srinivasan, K., & Somayaji, C. (2008). An Examination of Regenerative Organic Rankine Cycles Using Dry Fluids. *Applied Thermal Engineering*, *28*(8-9), 998–1007.

Meyer, L., Castillo, R., Buchgeister, J., & Tsatsaronis, G. (2010). Application of Exergoeconomic and Exergoenvironmental Analysis to an SOFC System with an Allothermal Biomass Gasifier. *International Journal of Thermodynamics*, *12*(4), 177–186.

Petrakopoulou, F., Tsatsaronis, G., & Morosuk, T. (2010). Conventional Exergetic and Exergoeconomic Analyses of a Power Plant with Chemical Looping Combustion for CO2 Capture. *International Journal of Thermodynamics*, *13*(3), 77–86.

Saleh, B., Koglbauer, G. Wendland, M., & Fischer, J. (2007). Working Fluids for Low-temperature Organic Rankine Cycles. *Energy, 32*(7), 1210–1221.

Schuster, A., Karellas, S., & Aumann, R. (2010) Efficiency Optimization Potential in Supercritical Organic Rankine Cycles. *Energy, 35*(2), 1033–1039.

Tchanche, B.F., Papadakis, G., Lambrinos, G., & Frangoudakis, A. (2009). Fluid Selection for a Low-temperature Solar Organic Rankine Cycle. *Applied Thermal Engineering*, *29*(11-12), 2468–2476.

Tsatsaronis, G., & Moran, M.J. (1997). Exergy-aided Cost Minimization. *Energy Conversion and Management Efficiency, Cost, Optimization, Simulation and Environmental Aspects of Energy Systems*, *38*(15-17), 1535–1542.

Tsatsaronis, G., & Winhold, M. (1985). Exergoeconomic Analysis and Evaluation of Energy-conversion plants — I. A New General Methodology. *Energy*, *10*(1), 69–80.

Turton, R., Bailie, R.C., & Whiting, W.B. (2003). *Analysis, Synthesis and Design of Chemical Processes*. (2nd ed.) Old Tappan, NJ: Prentice Hall.

Valero, A., Lozano, M.A. & Bartolomé, J.L. (1996). On-line Monitoring of Power-plant Performance, Using Exergetic Cost Techniques. *Applied Thermal Engineering, 16*(12), 933–948.

VDI-Gesellschaft Verfahrenstechnik und Chemieingenieurwesen (2006). *VDI-Wärmeatlas*. (10.ed.), Berlin, Springer Verlag.

Yari, M. (2010). Exergetic Analysis of Various Types of Geothermal Power Plants. *Renewable Energy*, *35*(1), 112–121.

Zaleta-Aguilar, A., Rangel-Hernandez, V. H., & Royo, J. (2010). Exergo-Economic Fuel-Impact Analysis for Steam Turbines Sections in Power Plants. *International Journal of Thermodynamics*, *6*(3), 133–141.